Non-existence of positive glitches in spectra using the YB_{66} double-crystal monochromator of BL15XU at SPring-8

Masaru Kitamura,[a]* Hideki Yoshikawa,[a] Takaho Tanaka,[a] Tetsuro Mochizuki,[b] Aurel Mihai Vlaicu,[a] Atsushi Nisawa,[a] Nobuhiro Yagi,[a] Masato Okui,[a] Masahiro Kimura[a] and Sei Fukushima[a]

[a]National Institute for Materials Science, BL15XU, SPring-8, 1-1-1 Koto, Mikazuki-cho, Sayo-gun, Hyogo 679-5198, Japan, and [b]Japan Synchrotron Radiation Research Institute, SPring-8, 1-1-1 Koto, Mikazuki-cho, Sayo-gun, Hyogo 679-5198, Japan. E-mail: masarukitamura@k3.dion.ne.jp

YB_{66} is suitable for dispersing synchrotron radiation in the 1–2 keV energy range with a $2d$ lattice spacing of 1.17 nm. When used with an undulator there are no positive glitches at 1385.6 and 1438 eV in spectra dispersed by a YB_{66} 400 double-crystal monochromator as observed using bending-magnet or wiggler beamlines. The transmission function of a YB_{66} double-crystal monochromator has been measured by means of a Si PIN photodetector, and X-ray absorption near-edge structure (XANES) of Mg, Al and Si were measured at high resolution. From all of these experiments it has been clarified that a YB_{66} double-crystal monochromator is well suited for soft X-ray beamlines on third-generation light sources.

Keywords: YB_{66}; double-crystal monochromators; glitches; XANES.

1. Introduction

We have adopted a YB_{66} double-crystal monochromator (Fukushima *et al.*, 1999) for use in the 1–2 keV energy range. YB_{66} has a f.c.c. packing structure of B_{156} units (Slack *et al.*, 1971, 1977), which has a lattice plane (400) whose large d-lattice spacing of 0.586 nm is suitable for dispersing soft X-rays (Tanaka *et al.*, 1985). Moreover, since YB_{66} is more resistant than other crystals (beryl, quartz, InSb) to synchrotron radiation damage (Wong *et al.*, 1982, 1999; Funabashi *et al.*, 1989) and has a higher resolution than other crystals, it is best suited for dispersing synchrotron radiation at a third-generation light source in the 1–2 keV energy range. On the other hand, YB_{66} has the disadvantages that its resolution is likely to be affected by the heat load because of its very low thermal conductivity (Slack *et al.*, 1971) and it exhibits non-uniform crystalline quality (Rek *et al.*, 1992). In addition, there are positive glitches at 1385.6 and 1438 eV in the spectrum dispersed by YB_{66} when using a bending magnet (Tanaka *et al.*, 1997; Wong *et al.*, 1999) or a wiggler (Kinoshita *et al.*, 1998).

The mechanism of positive-glitch generation was discussed by Tanaka *et al.* (1997), and it was confirmed that positive glitches are caused by sharp reflectivity increases associated with anomalous scattering for the 006 reflection at the Y L_3- and L_2-edges by means of reflectivity measurements and structure-factor calculations for the 006 reflections.

2. Experimental

YB_{66} crystals were installed in the double-crystal monochromator on the helical-undulator beamline B15XU at SPring-8 (Kitamura *et al.*, 2002, 2003). The experimental configuration is shown in Fig. 1. A helical undulator was adopted because the angular distribution of flux density is mainly distributed off the optical axis and power on the crystal is lower than that from a planar undulator (Hara *et al.*, 2001). Although a helical undulator decreases the thermal load compared with a planar undulator, additional thermal-load reduction is necessary with YB_{66} crystals (Avery, 1984; Bilderback, 1986 Bilderback *et al.*, 1986). The thermal load from a helical undulator was reduced by adjusting the aperture size of the front-end slit and adding a Be filter. Prior to using the YB_{66} crystal, the effects of power density and total power on the first YB_{66} crystal were evaluated using *SPECTRA* (Tanaka & Kitamura, 2001). The transmission function of the YB_{66} double-crystal monochromator was evaluated by measuring the photocurrent from a Si PIN photodetector at an experimental position while simultaneously scanning the monochromator and the helical undulator gap. XANES of Mg, Al and Si were also measured. The current before the sample was monitored with a Au mesh.

3. Results and discussion

The transmission function of the YB_{66} double-crystal monochromator is shown in Fig. 2. There are no positive glitches at 1385.6 and 1438 eV in the transmission function of the YB_{66} double-crystal monochromator of our undulator beamline. It is considered that this result supports the explanation of the glitch-generation mechanism in the previous study; positive glitches are generated due to the 006 reflection with an energy 1.5 times higher than that of the YB_{66} 400

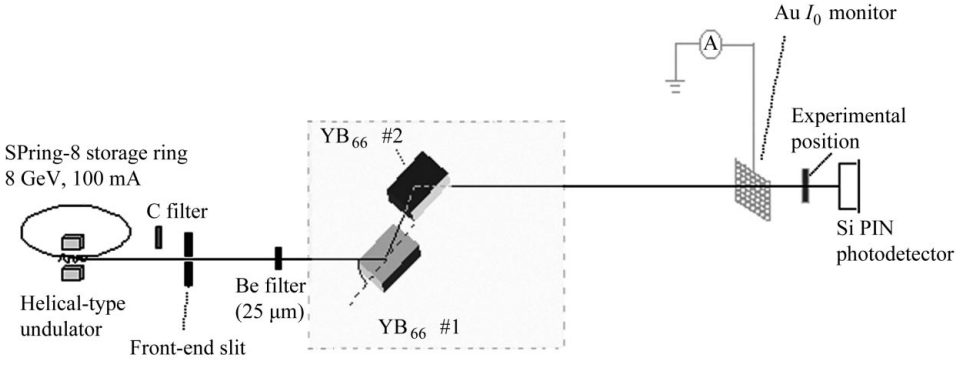

Figure 1
Outline of the experimental configuration to the first experimental hutch of beamline BL15XU at SPring-8. A tandem-type monochromator consists of two monochromators for which one can select an analyzer crystal from Si, YB_{66} and a multilayer. In the 1–2 keV energy range we adopted the YB_{66} crystal for dispersing synchrotron radiation.

reflection (Tanaka *et al.*, 1997). The spectrum from a helical undulator in the case of the first harmonics at 1385 eV calculated using *SPECTRA* is shown in Fig. 3(*a*). In the spectrum, the second harmonics are 2760 eV away from the photon energy of the Y L_3- and L_2-edges; the flux at 2080 eV corresponding to the Y L_3-edge was estimated to be 1.5×10^9 photons s^{-1} (0.1% bandwidth)$^{-1}$ (100 mA)$^{-1}$ with a Be filter (thickness 25 μm) and the flux at 2156 eV corresponding to the Y L_2-edge was estimated to be 1.8×10^9 photons s^{-1} (0.1% bandwidth)$^{-1}$ (100 mA)$^{-1}$ with a Be filter (thickness 25 μm). These flux values are three orders of magnitude smaller than that of the first harmonics with a Be filter (thickness 25 μm) and not sufficient to generate positive glitches.

Similarly, the spectrum from a helical undulator in the case of the first harmonics at 1438 eV calculated using *SPECTRA* is shown in Fig. 3(*b*). The flux at 2080 eV corresponding to the Y L_3-edge was estimated to be 1.2×10^9 photons s^{-1} (0.1% bandwidth)$^{-1}$ (100 mA)$^{-1}$ with a Be filter (thickness 25 μm) and the flux at 2156 eV corresponding to the Y L_2-edge was estimated to be 1.3×10^9 photons s^{-1} (0.1% bandwidth)$^{-1}$ (100 mA)$^{-1}$ with a Be filter (thickness 25 μm). These flux values are estimated to be four orders of magnitude smaller than that of the first harmonics with a Be filter (thickness 25 μm) and not sufficient to generate positive glitches. In the experiment using the YB_{66} crystals, a scan of the photon energy was performed by automatic tuning of a helical-undulator gap. Thus it is considered that the spectra of the first harmonics at 1385 and 1438 eV are the same as those estimated using *SPECTRA*.

From these discussions it is confirmed that positive glitches are not generated in the undulator beamline by automatic tuning of a helical-undulator gap. These results indicate that our undulator beamline effectively utilizes the YB_{66} 400 monochromator without the cut-off mirror which minimizes the intensity of anomalous high harmonics at glitches compared with using bending-magnet or wiggler beamlines.

To confirm that there were no positive glitches we measured XANES of Mg, Al and Si (Wong *et al.*, 1994, 1995). The results of the XANES measurements shown in Figs. 4, 5 and 6 clearly show the good normalization of the sample signal, I, by the input signal, I_0, with no glitches at 1385.6 or 1438 eV. In Fig. 4 the pre-edge at 1303 eV of Mg metal is observed clearly and the intermediate region between 1305 and 1309 eV is also shown clearly in the XANES. In Fig. 5 it is shown that the near-edge structure of Al metal has a hollow at approximately 1567 eV. Fig. 6 shows the near-edge structure of Si metal measured at a high resolution (Sham *et al.*, 1992). Kossel theoretically explained that the fine structure of the near edge is due to the excitation of inner-shell electrons to an unoccupied level (Kawai & Mayers, 2000). The Kossel theory is called the short-range-order theory because the electronic structures of unoccupied levels are mostly determined by hybridization between the centre atom and the nearest-neighbour atoms (Kawai & Mayers, 2000). Thus, we expect our undulator beamline BL15XU to provide users with substantial experimental data of electronic structures of unoccupied levels using the YB_{66} double-crystal monochromator at the third-generation light source SPring-8.

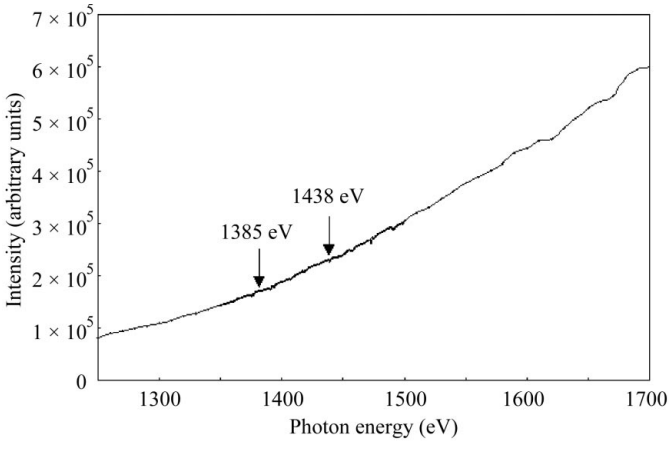

Figure 2
The transmission function of the YB_{66} double-crystal monochromator measured using the photocurrent of a Si PIN photodetector at an experimental position on the beamline. There are no positive glitches in the transmission function. Ring current = 100 mA, 25 μm Be filter, 0.04 mm × 0.6 mm front-end slit.

4. Conclusions

A double-crystal YB_{66} monochromator was constructed on a helical-undulator beamline at the third-generation light source SPring-8. It was confirmed that positive glitches do not appear in the transmission function of a YB_{66} 004 double-crystal monochromator. Furthermore, XANES of Mg, Al and Si were measured without a low-pass mirror filter. It is therefore possible to investigate the electronic structures of unoccupied levels of advanced materials with this undulator beamline. From these experiments it has been clarified that a YB_{66} double-crystal monochromator is well suited for soft X-ray beamlines on third-generation light sources.

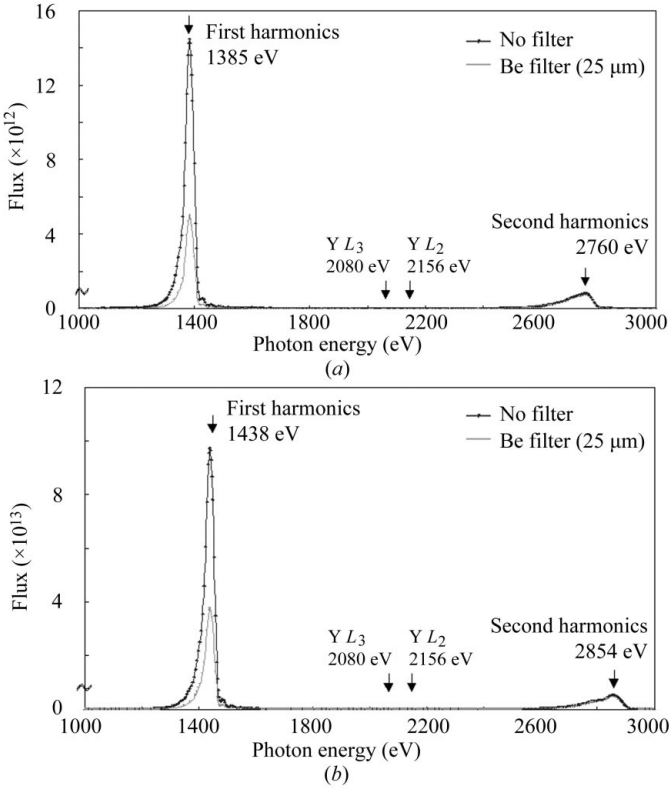

Figure 3
Spectrum of the first harmonics at (*a*) 1385 eV and (*b*) 1438 eV from a helical undulator of BL15XU calculated using *SPECTRA*. Ring current = 100 mA, 0.04 mm × 0.6 mm front-end slit. The flux is measured in units of photons s^{-1} (0.1% bandwidth)$^{-1}$ (100 mA)$^{-1}$.

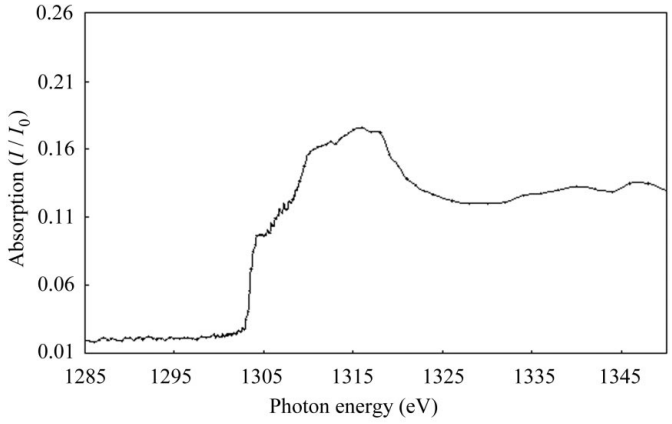

Figure 4
XANES of Mg metal. The pre-edge at 1303 eV is clearly observed and the intermediate region between 1305 and 1309 eV is also shown clearly.

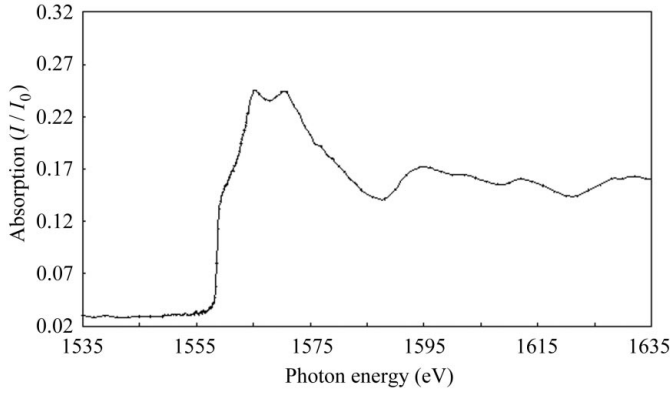

Figure 5
XANES of Al metal. It is shown that the near-edge structure has a hollow at approximately 1567 eV.

The authors thank Dr J. Wong, Lawrence Livermore National Laboratory, and Dr M. Rowen and Dr Z. U. Rek, Stanford Synchrotron Radiation Laboratory, for their useful advice.

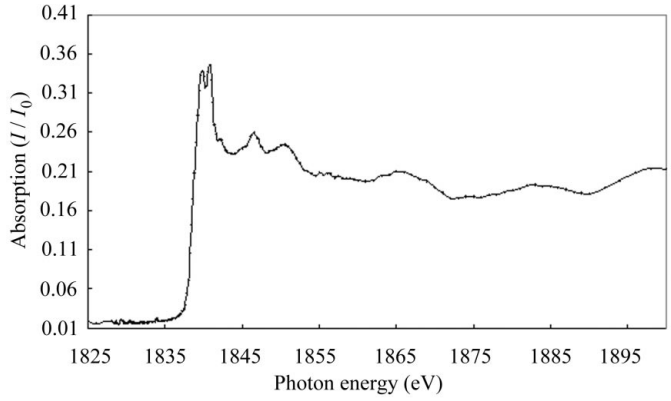

Figure 6
XANES of Si metal. It is shown that the near-edge structure of Si metal is measured at high resolution.

References

Avery, R. T. (1984). *Nucl. Instrum. Methods*, **222**, 146–158.
Bilderback, D. H. (1986). *Nucl. Instrum. Methods*, A**246**, 434–436.
Bilderback, D. H., Mills, D. M., Batterman, B. W. & Henderson, C. (1986). *Nucl. Instrum. Methods*, A**246**, 428–433.
Fukushima, S., Yoshikawa, H., Nisawa, A., Kitamura, M., Kohiki, S., Okamura, F. P., Kimura, M., Okui, M., Mizutani, T. & Yagi, N. (1999). NIRIM Annual Report, pp. 48–49. National Institute for Research in Inorganic Materials, Tsukuba, Ibaraki, Japan.
Funabashi, M., Nomura, M., Kitajima, Y., Yokoyama, T., Ohta, T. & Kuroda, H. (1989). *Rev. Sci. Instrum.* **60**, 1983–1986.
Hara, T., Tanaka, T., Seike, T., Bizen, T., Maréchal, X., Nisawa, A., Fukushima, S., Yoshikawa, H. & Kitamura, H., (2001). *Nucl. Instrum. Methods*, A**467/468**, 161–164.
Kawai, J. & Mayers, R. A. (2000). Editors. *Encyclopedia of Analytical Chemistry*, pp. 13288–13315. Chichester: John Wiley.
Kinoshita, T., Takata, Y., Matsukawa, T., Aritani, H., Matsuo, S., Yamamoto, T., Takahashi, M., Yoshida, H., Yoshida, T., Ufuktepe, Y., Nath, K. G., Kimura, S. & Kitajima, Y. (1998). *J. Synchrotron Rad.* **5**, 726–728.
Kitamura, M., Yoshikawa, H., Mochizuki, T., Vlaicu, A. M., Nisawa, A., Yagi, N., Okui, M., Kimura, M., Tanaka, T. & Fukushima, S. (2002). *Adv. X-ray Anal.* In the press.
Kitamura, M., Yoshikawa, H., Mochizuki, T., Vlaicu, A. M., Nisawa, A., Yagi, N., Okui, M., Kimura, M., Tanaka, T. & Fukushima, S. (2003). *Nucl. Instrum. Methods*, A**497**, 550–562.
Rek, Z. U., Wong, J., Tanaka, T., Kamimura, Y., Schäfers, F., Müller, B., Krumrey, M. & Müller, P. (1992). *Proc. SPIE*, **1740**, 173–180.
Sham, T. K., Feng, X. H., Jiang, D. T., Yang, B. X., Xiong, J. Z., Bzowski, A. B., Houghton, D. C., Bryskiewicz, B. & Wang, E. (1992). *Can. J. Phys.* **70**, 813–818.
Slack, G. A., Oliver, D. W., Brower, G. D. & Young, J. D. (1977). *J. Phys. Chem. Solids*, **38**, 45–49.
Slack, G. A., Oliver, D. W. & Horn, F. H. (1971). *Phys. Rev. B*, **4**, 1714–1720.
Tanaka, T., Aizawa, T., Rowen, M., Rek, Z. U., Kitajima, Y., Higashi, I., Wong, J. & Ishizawa, Y. (1997). *J. Appl. Cryst.* **30**, 87–91.
Tanaka, T. & Kitamura, H. (2001). *J. Synchrotron Rad.* **8**, 1221–1228.
Tanaka, T., Otani, S. & Ishizawa, Y. (1985). *J. Cryst. Growth*, **73**, 31–36.
Wong, J., George, G. N., Pickering, I. J., Rek, Z. U., Rowen, M., Tanaka, T., Via, G. H., DeVries, B., Vaughan, D. E. W. & Brown, G. E. Jr (1994). *Solid State Commun.* **92**, 559–562.
Wong, J., Rek, Z. U., Rowen, M., Tanaka, T., Schäfers, F., Müller, B., George, G. N., Pickering, I. J., Via, G., DeVries, B., Brown, G. E. Jr & Föba, M. (1995). *Physica B*, **208/209**, 220–222.
Wong, J., Roth, W. L., Batterman, B. W., Berman, L. E., Pease, D. E., Heald, S. & Barbee, T. (1982). *Nucl. Instrum. Methods*, **195**, 133–139.
Wong, J., Tanaka, T., Rowen, M., Schäfers, F., Müller, B. R. & Rek, Z. U. (1999). *J. Synchrotron Rad.* **6**, 1086–1095.